Effect of insulating barrier on rectification, injection and transport properties of printed organic diodes.

K E Lilja[1,4], H S Majumdar[2], K Lahtonen[3], P Heljo[1], S Tuukkanen[1], T Joutsenoja[1], M Valden[3], R Österbacka[2] and D Lupo[1]

[1]Tampere University of Technology, Department of Electronics, P.O. Box 692, FI-33101 Tampere, Finland

[2]Åbo Akademi University, Department of Natural Science and Center for Functional Materials, Porthansgatan 3, FI-20500, Turku, Finland

[3]Tampere University of Technology, Surface Science Laboratory, P.O. Box 692, FI-33101 Tampere, Finland

E-mail: kaisa.lilja@tut.fi

[4]Author to whom any correspondence should be addressed.

Abstract. Rectification ratios of 10^5 were observed in printed organic copper/polytriarylamine/silver diodes when a thin insulating barrier layer was inserted at the cathode interface. To clarify the origin of the high rectification ratio in the diodes, the injection, transport and properties of the diodes with two different copper cathodes were examined using impedance spectroscopy and X-ray photoelectron spectroscopy (XPS). The impedance data confirm that the difference in the diode performance arises from the copper interface. The XPS measurements show that the copper surface in both diode structures was covered by a layer of Cu_2O topped by an organic layer. The organic layer was thicker on one of the surfaces, which resulted in lower reverse currents and higher rectification ratios in printed diodes. We suggest a model where a dipole at the dual insulating layer induces a shift in the semiconductor energy levels explaining the difference between the diodes with different cathodes.

1. Introduction

The foreseen advantages of organic semiconductor materials rely on the possibility to fabricate electronic components and circuits using cost-effective manufacturing processes. This requires solution processable materials and fundamental research on organic electronic components, such as

diodes and transistors. Previously, high-throughput gravure printing processes have been demonstrated for organic light emitting diodes and transistors. [1-4] Also, gravure printed organic Schottky diodes have been demonstrated as RFID rectifiers and as the active components in display driving circuitry. [5, 6] In these applications, the organic diode needs to exhibit a sufficient rectification ratio and forward current.

Recently it has been shown that processing and device architecture have a significant effect on the performance of printed organic Schottky diodes. [9] The diodes exhibited very low currents under reverse bias despite the low Schottky barrier. Furthermore, a thin interfacial barrier layer was found to prevent hole injection from the cathode electrode into the organic semiconductor under reverse bias without having a significant effect on the forward bias current, leading to a higher rectification ratio. It is unlikely that a Schottky barrier as low as 0.1 eV to 0.3 eV, albeit combined with a tunnelling barrier, could completely explain rectification ratios of 10^3 to 10^5. In this article we clarify the origin of the high rectification of the diodes and their improvement upon adding an additional dielectric layer.

The interfacial phenomena at metal-organic interfaces have been described in detail both from theoretical and modelling perspectives.[10, 11] One of the most important effects in determining the electrical structure of the contact is Fermi-level pinning of the semiconductor. Here, we verify the different behaviour of two diode structures by using impedance spectroscopy, which has been used by several groups to study the behaviour of metal/organic interfaces and interfacial layers in organic (light-emitting) diode structures. [12-16] X-ray photoelectron spectroscopy (XPS) is a well-known characterization method for determining the chemical composition and depth distribution of elements on the surface of various materials. We use XPS to find detailed information on the composition of the diode cathode interface by examining the Cu LMM transitions and the depth profile of the copper electrodes. Based on these results, the previously presented model for charge carrier movement across the barrier layer at the cathode interface is extended and the origin of the high rectification ratio in these diodes discussed.

2. Material and methods

The diodes were fabricated using roll-to-roll compatible printing processes. A copper cathode layer was either vacuum evaporated or sputtered onto a poly(ethylene terephthalate) (PET) film and patterned by shadow masking or wet etching. The polytriarylamine semiconductor (PTAA) layer, and anode (silver) inks were printed with a laboratory-scale gravure printing press (Labratester Automatic from Norbert Schläfli Maschinen) and cured at 115 ºC. The diodes were fabricated in a dust-free environment (close to ISO 14644-1 class 5) at room temperature.

The dc current density - voltage (J-V) -characteristics of the diodes were measured using a Keithley 236 Source-Measure Unit under ambient laboratory conditions. The diode capacitances were measured using a HP 8752A Network Analyzer at a frequency of 10 MHz and 22 mV rms. Impedance spectroscopy was done with a Gamry 600™ Potentiostat in a frequency range of 10Hz to 1 MHz. The amplitude of the ac bias was 20 mV rms. The dc bias was varied from 0.1 V to 5.0 V.

The chemical composition and thicknesses of the surface layers on the copper cathodes were analyzed utilizing nonmonochromatized dual anode X-ray photoelectron spectrometer (ESCA3000 XPS, VG Microtech Inc., UK) located in an ultrahigh vacuum (UHV) system with a base pressure of $<1\times10^{-10}$ mbar. The UHV system is described in detail elsewhere. [17] The XPS measurements were performed at 0° emission angle and Al Kα radiation was utilized for excitation. The elemental concentrations were determined from a circular detection area of ~600 μm in diameter on patterned metal substrates that had been stored under ambient laboratory conditions prior to measurement. Both, the XPS survey spectra and the Cu LMM transitions were analysed. The analysis procedure of the Cu LMM transition is described elsewhere in more detail [18]. The inelastic electron energy-loss background thickness analysis was performed with QUASES software package, [19] using reference spectra of experimentally obtained line shapes of metallic Cu, Cu_2O, and PET. The error of the inelastic electron energy-loss background analysis method is ±10% in coverage and ±20% in thickness.

3. Results and Discussion

The log J- log V -characteristics of the diodes with evaporation-deposited (Cu(e)) and sputter-deposited (Cu(s)) copper cathodes are presented in figure 1. The diodes are under forward bias when the silver electrode is biased positively with respect to the copper electrode. For Cu(e) diodes the current turns to space-charge limited at around an applied voltage of 0.2 V. For Cu(s) diodes the current is injection limited up to about 2 V, above which the current approaches space-charge limited behaviour. Furthermore, the rectification ratio improves from 10^3 to 10^5 due to the lower reverse current of the diodes with sputtered copper cathodes. Since there are no other differences between the diode structures except for the copper electrode, it is suggested that interfacial effects at the copper interface play a role up to at least 2 V in the Cu(s) diodes.

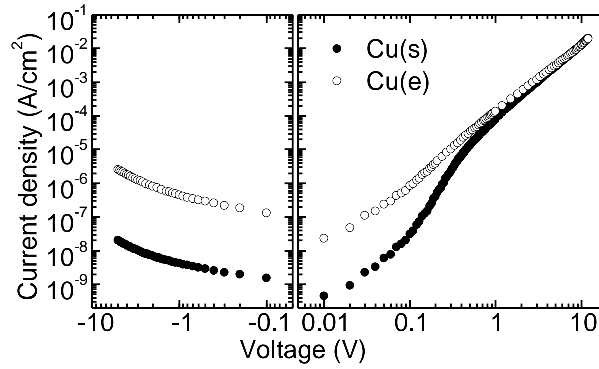

Figure 1. Log J- log V -performance of diodes with sputtered [Cu(s)] and evaporated [Cu(e)] copper cathodes.

In conventional inorganic metal-semiconductor (MS) diodes, a thin depletion region forms at the cathode interface of the diode. However, since organic semiconductors exhibit low charge carrier concentrations and thus low conductivities, the depletion region can expand throughout the thickness of the semiconductor. [7, 8] In conventional MS -diodes the width of the depletion layer W is given by

$$W = \sqrt{\frac{2\varepsilon_0 \varepsilon_r (V_{bi} - V)}{qN_A}} \tag{1}$$

Where ε_0 is the permittivity of vacuum, ε_r is the permittivity of the semiconductor, V_{bi} the built-in potential, V the applied voltage, q the elementary charge and N_A the density of dopants. [20] When the formula is applied for an organic semiconductor, N_A can be equated to the density of free charge n, and V_{bi} to the work function difference between the anode and the cathode. [7]

The density of free charge can be calculated from

$$J = \frac{qn\mu V}{d} \tag{2}$$

Where d is the semiconductor thickness [8]. Using the semiconductor mobility 1.4×10^{-3} $cm^2/(V\ s)$ that can be calculated from the space-charge limited region of the J - V characteristics using $\varepsilon_r = 3$ and the semiconductor thickness 1.5 μm, [9] the depletion region in the Cu(s) diodes can be estimated to be several micrometers wide at an applied voltage of 0.01 V. This is much more than the thickness (1.5 μm) of the semiconductor, which implies that the diode is fully depleted. Thus, the diode behaviour cannot be predicted using the model for conventional inorganic diodes with a thin depletion region. Instead, the diode energy levels are illustrated with tilted, rigid bands. Since the Schottky barrier in the diodes is only 0.1 eV to 0.3 eV for Cu(s) and Cu(e) diodes, respectively [9], we argue that an additional interfacial effect is responsible for the observed high rectification ratios.

Impedance spectroscopy was used to demonstrate that the difference in transport characteristics of the diodes is due to the metal-/semiconductor interface. Measurements were done on Cu(e) and Cu(s) diodes in a frequency range of 10 Hz to 1 MHz. Additionally, the diode capacitances were measured at 10 MHz using the HP 8752A Network Analyzer. At MHz frequencies only the bulk capacitance of the semiconductor is observed. It was found that the bulk capacitances were the same for both diodes. However, the impedance data revealed differences that concurred with the J-V -characteristics. Figure 2 shows the cole-cole plots Cu(e) (open circle) and Cu(s) (closed circle) diodes. The frequency in the plots increases from right to left. For a dc bias of 5.0 V there was no difference between the impedance of the diodes (figure 2(a)), but as the dc bias was decreased a distinct difference was observed. As seen also in the J-V -data, a difference between the diodes started to appear with voltages below ~0.5 V. In the impedance data, the difference systematically increased for dc biases of 0.4 V (figure 5(b)), 0.2 V (figure 5(c)) and 0.1 V (figure 5(d)). The important observation from the impedance data and from the capacitance measurement is that though the bulk capacitance of the semiconductor layer in the diode did not change, the overall impedance of the diodes varied as a function of the applied bias voltage. Since the only difference between the diodes is the interface between the semiconductor and the copper, it is safe to conclude that the impedance difference between the diodes is from the variation of the cathode interface. The fact that the difference is most pronounced at the low frequency region also corroborates with the fact that the variation is an interfacial effect.

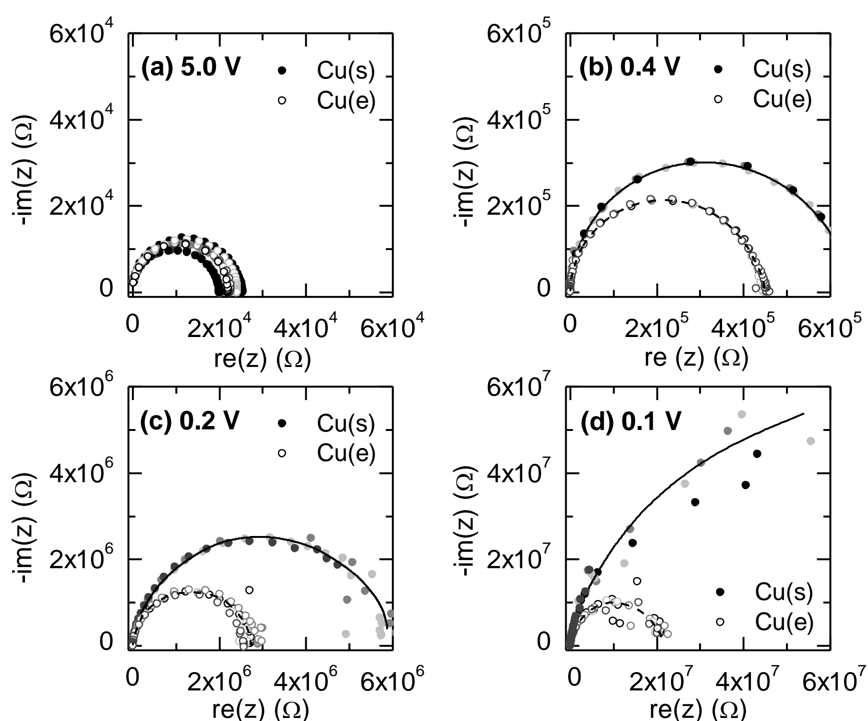

Figure 2. Cole-cole plots of the diode impedance with and sputtered [Cu(s), closed circle] and evaporated [Cu(e), open circle] cathode contacts at forward bias voltages of 0.1 V, 0.2 V, 0.4 V and 5.0 V. The frequency increases from right to left from 10 Hz to 1 MHz.

Efforts were made to fit the experimental impedance data to formulate an equivalent circuit for the diode structures. It was possible to reasonably fit the data for 5.0 V dc bias with one parallel RC circuit that represented only the PTAA bulk. Whereas the real capacitance value obtained for the bulk agreed with the capacitance value obtained from high frequency measurements, it was not possible to find a suitable equivalent circuit for the diodes at low dc bias. This is most likely due to the pronounced role of the interfaces on injection and transport at low biases as well as parasitic capacitances from measurement wires and printed conductor lines. Also, the conductivity and/or dielectric constant of the semiconductor can be frequency dependent which complicates the RC fitting using simple RC elements. [13]

Previously we observed indications of an organic layer covering the surface of the Cu(s) substrate. [9] This analysis was based on a survey spectrum of the XPS signal intensity with binding energies from 0 to 1100 eV. Here we report the results based on more detailed XPS study, including analysis of the surface in-depth chemical structure and copper oxidation state obtained from Cu LMM transitions. Figure 3 represents survey spectra and Cu LMM transitions of the Cu(e) and Cu(s) surfaces. As shown in figure 3(a), the Cu(s) surface contained higher relative concentration of carbon and attenuated copper signals. The results are comparable to earlier results and suggest that the Cu(s) surface is covered by an organic layer. Carbon is also detected on the Cu(e) surface where the copper signals are stronger indicating carbon impurities on top of the surface.

The X-ray excited Auger peaks of copper at 568.3, 568.8 and 570.0 eV can be assigned to metallic Cu, Cu (II) and Cu (I) -oxidation states, respectively. The $L_3M_{45}M_{45}$ transitions of the Cu(e) and Cu(s) surfaces are shown in figure 3(b). The copper is mostly as Cu (I), presumably as Cu_2O, since the substrates are stored in ambient air after fabrication. The shapes of the Cu LMM transition and shake-up satellites of the Cu 2p (not shown) indicate that Cu (II) is not present on either surface. The sampling depth of the Cu LMM signal through the Cu_2O and organic layer is in the order of 6–7 nm. On both surfaces the metallic Cu LMM signal is observed. Thus, if uniform layer thicknesses are assumed, the metallic Cu layer is buried less than 7 nm deep below the other layers.

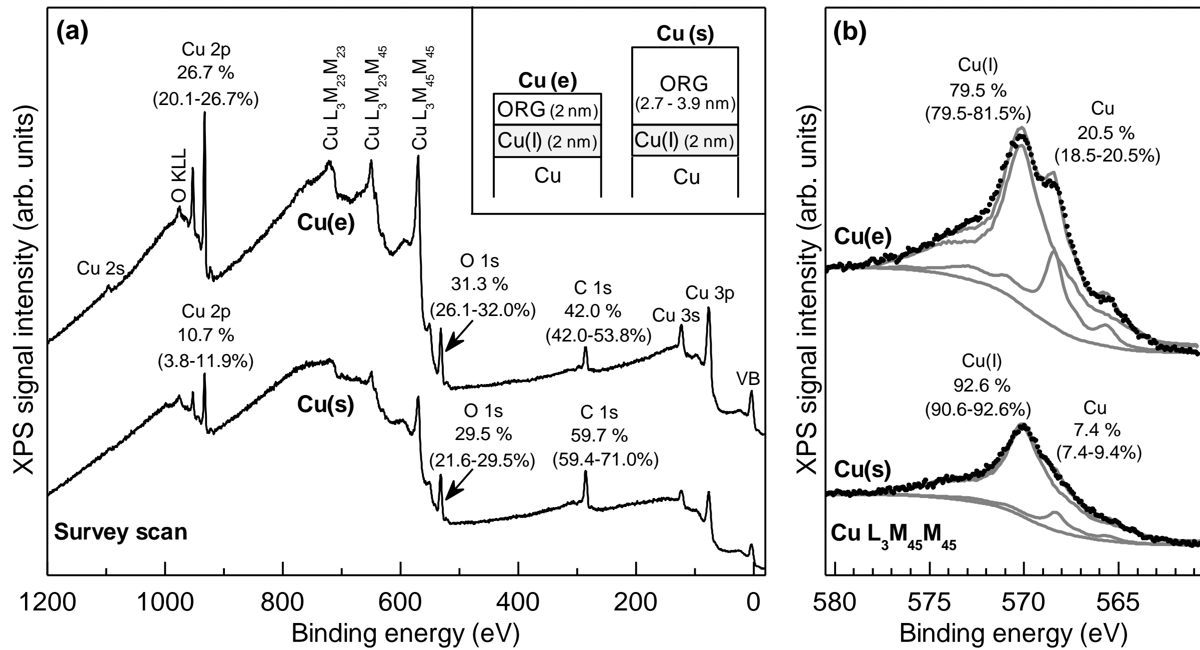

Figure 3. (a) Survey spectra and (b) Cu $L_3M_{45}M_{45}$ transitions of the evaporated [Cu(e)] and sputtered [Cu(s)] surfaces. The atomic concentrations of Cu, O, and C are indicated in the figure. The upper values are for the shown spectra. The values in brackets indicate the variation range of four different non-overlapping positions on the samples. The inset shows a schematical presentation of the surface layers, where ORG is the organic layer and Cu(I) is the Cu_2O layer on top of the metallic copper.

More accurate layer thicknesses on the copper surfaces were calculated based on the analysis of the inelastic electron energy-loss backgrounds and main peaks of the Cu 2p and C KVV transitions. According to the in-depth chemical analysis, the thickness of the organic layer (ORG) on Cu(s) varied between 2.7 and 3.9 nm, and the thickness of the Cu_2O layer was 2 nm, as presented in the inset of figure 3. Using the same reference spectra for Cu(e), the thickness of the organic layer was 2 nm and Cu_2O layer 2 nm. The exploited buried layer morphology model is simplified, and quality of the fitting was lower with Cu(e), indicating that the actual layer thickness is not absolutely uniform and the layer may have pinholes or island formation.

Since the J-V characteristics in figure 1 show that the rectification ratio is higher with Cu(s), the Schottky barriers (0.3 eV and 0.1 eV for Cu(e) and Cu(s), respectively) cannot explain the difference. We argue that the difference between the diodes is due to the observed interfacial layer on the cathode contact. In fact, *both* the organic layer and the Cu_2O layer are likely to have an effect on the charge carrier movement across the cathode interface. The prior hypothesis for the diode function in reverse bias was that the semiconductor is fully depleted and there are no charge carriers that could create a sufficient field across the interfacial barrier to assist tunnelling through the barrier, thus the reverse current in the Cu(s) diodes is very low. [9] Based on the XPS and impedance data the hypothesis can

be extended using the dual (Cu_2O + organic) insulating layer, as presented in figure 4. Since the measured Schottky barrier Φ_B, determined as the difference between the metal work function Φ_M and the HOMO of the semiconductor, is as low as 0.1 - 0.3 eV, as presented in figure 4(a), it is probable that an additional contact effect induces a higher Schottky barrier once the copper and the semiconductor are brought into contact (figures 4 (b-e)). This can be understood as pinning of the semiconductor Fermi-level which has been extensively explained both for organic and inorganic semiconductor materials and is caused either by wave functions of electrons in the metal that tail into the semiconductor or by bond polarization. [21,10,11] In practice this means that close contact between a metal and a semiconductor will cause the semiconductor energy levels to pin at a certain level. An insulator between the materials will cause a change in the pinning. As illustrated in figure 4(b), this causes an increase in the Schottky barrier. When the Schottky barrier is increased, a few charge carriers flow from the copper to the semiconductor under reverse bias and the reverse current is low, which improves the rectification ratio to 10^3.

It has been shown for inorganic semiconductors that using a dual layer of a dielectric and an oxide will cause a dipole at the insulator-oxide interface. [21,22] This dipole induces a barrier shift and can be visualised as modifying the interface energetics. Since the XPS data show that there is a dual layer of Cu_2O and organic material on the copper surface, we argue that an interfacial dipole which modifies (or pins) the effective highest occupied molecular orbital (HOMO) of the semiconductor close to the interface is formed at the cathode interface of the Cu(s) diodes. The effect of the dipole in reverse bias is presented in figure 4(c). Due to the high Schottky barrier, only few charge carriers are able to flow from the copper to the semiconductor under reverse bias and the reverse current is very low, leading to a high rectification ratio of 10^5. However, as argued in previous work [9], in forward bias the field is still high enough to assist tunnelling through the barrier, as illustrated in figure 4(d) and (e).

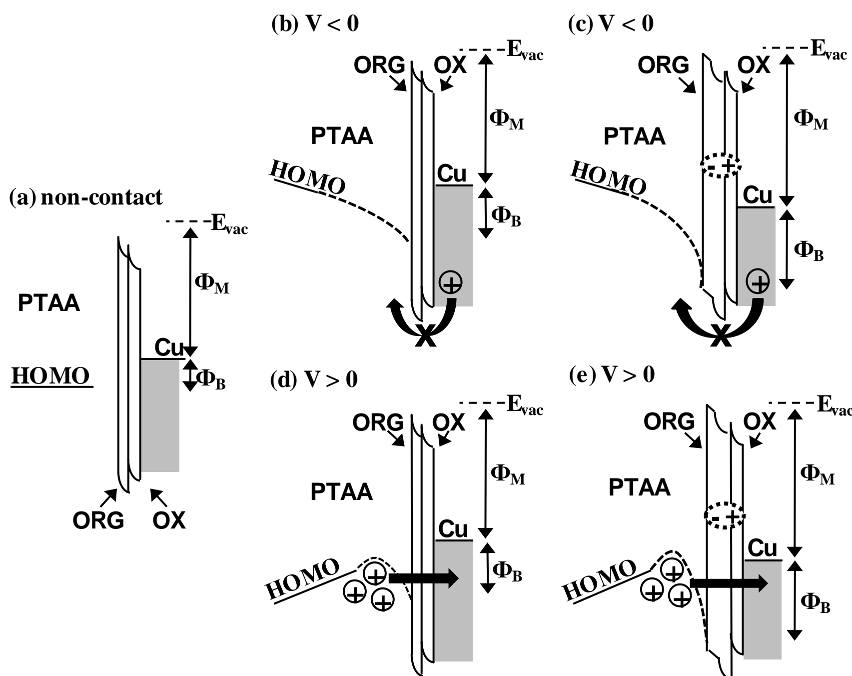

Figure 4. Simplified model for the Schottky contact. E_{vac} is the vacuum energy level. Φ_M is the metal work function in vacuum and Φ_B is the potential (Schottky) barrier. OX represents the Cu(I)-oxide and ORG represents the organic layer on top of the Cu(s) surface.

4. Conclusions

In conclusion, the effect of an insulating barrier on the rectification ratio, injection and transport properties of printed organic Schottky diodes was examined. Impedance spectroscopy and XPS results show that the insulating layer consists of Cu_2O and organic material. An organic layer with a thickness of 3 - 4 nm in the Cu(s) diodes lowers the diode reverse current by 2 orders of magnitude compared to an organic layer of 2 nm in the diodes with evaporated copper cathodes. Since the semiconductor is fully depleted under reverse bias, there is no sufficient field across the interfacial barrier to assist tunnelling through the barrier and reverse current in the diodes is very low. Furthermore, we argue that an interfacial dipole in the dual insulator layer amplifies the barrier effect by causing a shift in the semiconductor energy levels. As a result, organic diodes with low reverse currents and rectification ratios of 10^5 were printed.

Acknowledgments

The authors acknowledge UPM-Kymmene Corporation for financial support.

References

[1] Kopola P, Tuomikoski M, Suhonen R and Maaninen A 2009 *Thin Solid Films* **517** 5757-62

[2] Hambsch M, Reuter K, Stanel M, Schmidt G, Kempa H, Fügmann U, Hahn U and Hübler A C 2010 *Mat. Sci. Eng. B* **170** 93-98

[3] Chung D-Y, Huang J, Bradley D D C and Campbell A J 2010 *Org. Electron.* **11** 1088-95

[4] Vornbrock A de la F, Sung D, Kang H, Kitsomboonloha R and Subramanian V 2010 *Org. Electron.* **11** 2037-44

[5] Lilja K E, Bäcklund T G, Lupo D, Hassinen T and Joutsenoja T 2009 *Org. Electron.* **10** 1011-14

[6] Lilja K E, Bäcklund T G, Lupo D, Virtanen J, Hämäläinen E and Joutsenoja T 2010 *Thin Solid Films* **518** 4385-89

[7] Braga D, Campione M, Borghesi A and Horowitz G 2010 *Adv. Mater.* **22** 424-8

[8] Campbell A J, Bradley D D C and Lidzey D G 1997 *J. Appl Phys.* **82** 6326-42

[9] Lilja K E, Majumdar H S, Pettersson F S, Österbacka R and Joutsenoja T 2011 *ACS Appl. Mater. Interfaces* **3** 7-10

[10] Braun S, Salaneck W R and Fahlman M 2009 *Adv. Mater.***21** 1450-72

[11] Ishii H, Sugiyama K, Ito E and Seki K 1999 *Adv. Mater.* **11** 605-25

[12] Taylor D M and Gomes H L 1995 *J. Phys. D: Appl. Phys.* **28** 2554-68

[13] Meier M, Karg S and Riess W 1997 *J. Appl. Phys.* **82** 1961-66

[14] Scherbel J, Nguyen P H, Paasch G, Brütting W and Schwoerer M 1998 *J. Appl. Phys.* **83** 5045-55

[15] Drechsel J, Pfeiffer M, Zhou X, Nollau A and Leo K 2002 *Synth. Metals* **127** 201-5

[16] Kim S H, Jang J W, Lee K W, Lee C E and Kim S W 2003 *Solid State Commun.* **128** 143-6

[17] Lahtonen K, Lampimäki M, Jussila P, Hirsimäki M and Valden M 2006 *Rev. Sci. Instrum.* **77** 083901

[18] Lampimäki M, Lahtonen K, Hirsimäki M and Valden M 2007 *Surf. Interface Anal.* **39** 359-66

[19] Tougaard S 2003 *QUASES: Software for quantitative XPS/AES of surface nanostructures by analysis of the peak shape and background (Version 5.0)* (Odense, Denmark: University of Southern Denmark) http://www.quases.com

[20] Sze SM and Ng K K 2007 *Physics of Semiconductor Devices* 3rd edn, (USA: John Wiley & Sons) p 137

[21] Hu J, Wong H-S P and Saraswat K 2011 *MRS Bulletin* **36** 112-9

[22] Coss B E, Loh W-Y, Wallace R M, Kim J, Majhi P and Jammy R 2009 *Appl. Phys. Lett.* **95** 222105